

the un replenished inner disk to drain viscously onto the star in a short timescale. Studies of the ultraviolet and H α flux arising from the accretion process, and near-infrared flux from the inner disk, suggest that a significant fraction of T Tauri stars are able to dissipate their inner disks rapidly⁷. Related processes may be relevant to the formation of planetary satellite systems¹².

For planetary formation, these results imply that steady growth of giant planets in massive disks around solar mass stars is limited by the vulnerability of the disk to fragmentation once the planetary mass reaches approximately 5 Jupiter masses. The resulting formation of additional planets, which then compete to accrete the available disk gas, implies an upper limit to the mass of massive planets formed by this mechanism. In particular, even if the disk was sufficiently massive it would not be possible to grow a planet from a Jupiter mass far into the brown dwarf regime. This is consistent with observational evidence that planets and brown dwarfs do not share a common mass function¹, which has prompted suggestions that a break in formation mechanisms exists at around 7 Jupiter masses. Finally we note that the endpoint of early disk fragmentation would be a system of numerous massive coplanar planets in initially close-to-circular orbits. Such a system would possess a global organisation imprinted via non-local gravitational effects at birth. These would be favourable initial conditions for the eventual formation of a system comprising one or more massive planets on eccentric orbits⁹. □

Received 25 May; accepted 15 October 1999.

1. Mayor, M., Udry, S. & Queloz, D. in *The Tenth Cambridge Workshop on Cool Stars, Stellar Systems and the Sun* (eds Donahue, R. A. & Bookbinder, J. A.) 77–87 (ASP Conf. Ser. 154, San Francisco, 1998).
2. Marcy, G. W. & Butler, R. P. Detection of extrasolar giant planets. *Annu. Rev. Astron. Astrophys.* **36**, 57–98 (1998).
3. Lin, D. N. C., Bodenheimer, P. & Richardson, D. C. Orbital migration of the planetary companion of 51 Pegasi to its present location. *Nature* **380**, 606–607 (1996).
4. Murray, N., Hansen, B., Holman, M. & Tremaine, S. Migrating planets. *Science* **279**, 69–72 (1998).
5. Rasio, F. A. & Ford, E. B. Dynamical instabilities and the formation of extrasolar planetary systems. *Science* **274**, 954–965 (1996).
6. Weidenschilling, S. J. & Marzari, F. Gravitational scattering as a possible origin for giant planets at small stellar distances. *Nature* **384**, 619–621 (1996).
7. Strom, S. E. Initial frequency, lifetime and evolution of YSO disks. *Rev. Mex. Astron. Astrophys. Ser. Conf.* **1**, 317–328 (1995).
8. Gladman, B. Dynamics of systems and two close planets. *Icarus* **106**, 247–263 (1993).
9. Lin, D. N. C. & Ida, S. On the origin of massive eccentric planets. *Astrophys. J.* **477**, 781–791 (1997).
10. Artymowicz, P. & Lubow, S. H. Mass flow through gaps in circumbinary disks. *Astrophys. J.* **467**, L77–L80 (1996).
11. Takeuchi, T., Miyama, S. M. & Lin, D. N. C. Gap formation in protoplanetary disks. *Astrophys. J.* **460**, 832–847 (1996).
12. Lin, D. N. C. & Papaloizou, J. On the structure of circumbinary accretion discs and the tidal evolution of commensurable satellites. *Mon. Not. R. Astron. Soc.* **188**, 191–201 (1979).
13. Kley, W. Mass flow and accretion through gaps in accretion discs. *Mon. Not. R. Astron. Soc.* **303**, 696–710 (1999).
14. Bryden, G., Chen, X., Lin, D. N. C., Nelson, R. P. & Papaloizou, J. C. B. Tidally induced gap formation in protostellar disks: Gap clearing and suppression of protoplanetary growth. *Astrophys. J.* **514**, 344–367 (1999).
15. Safronov, V. S. *Evolution of the Protoplanetary Cloud and Formation of the Earth and the Planets* (Izdatel'stvo Nauka, Moscow, 1969). (English translation for NASA and NSF by Israel Program for Scientific Translations, Jerusalem, NASA-TT-F-677, 1972).
16. Boss, A. P. Evolution of the solar nebula IV. Giant gaseous protoplanet formation. *Astrophys. J.* **503**, 923–937 (1998).
17. Osterloh, M. & Beckwith, S. V. W. Millimeter-wave continuum measurements of young stars. *Astrophys. J.* **439**, 288–302 (1995).
18. Hayashi, C., Nakazawa, K. & Nakagawa, Y. in *Protostars and planets II* (eds Black, D. C. & Matthews, M. S.) 1100–1153 (Univ. Arizona Press, Tucson, 1985).
19. Balbus, S. A., Hawley, J. F. & Stone, J. M. Nonlinear stability, hydrodynamical turbulence, and transport in disks. *Astrophys. J.* **467**, 76–86 (1996).
20. Larson, R. B. Gravitational torques and star formation. *Mon. Not. R. Astron. Soc.* **206**, 197–207 (1984).
21. Lin, D. N. C. & Pringle, J. E. The formation and initial evolution of protostellar disks. *Astrophys. J.* **358**, 515–524 (1990).
22. Toomre, A. On the gravitational stability of a disk of stars. *Astrophys. J.* **139**, 1217–1238 (1964).
23. Laughlin, G. & Bodenheimer, P. Nonaxisymmetric evolution in protostellar disks. *Astrophys. J.* **436**, 335–354 (1994).
24. Nelson, A. E., Benz, W., Adams, F. C. & Arnett, D. Dynamics of circumstellar disks. *Astrophys. J.* **502**, 342–371 (1998).
25. Lissauer, J. J. Timescales for planetary accretion and the structure of the protoplanetary disk. *Icarus* **69**, 249–265 (1987).
26. Pollack, J. B. *et al.* Formation of the giant planets by concurrent accretion of solids and gas. *Icarus* **124**, 62–85 (1996).
27. Shakura, N. I. & Sunyaev, R. A. Black holes in binary systems. Observational appearance. *Astron. Astrophys.* **24**, 337–355 (1973).

28. Benz, W. in *The Numerical Modelling of Nonlinear Stellar Pulsations* (ed. Buchler, J. R.) 269–287 (Kluwer Academic, Dordrecht, 1990).
29. Monaghan, J. J. Smoothed particle hydrodynamics. *Annu. Rev. Astron. Astrophys.* **30**, 543–574 (1992).
30. Barnes, J. & Hut, P. A hierarchical O(N log N) force calculation algorithm. *Nature* **324**, 446 (1986).

Acknowledgements

We thank N. Murray for helpful discussions, and N. Wilson for maintaining the required computational resources.

Correspondence and requests for materials should be addressed to P. Armitage (e-mail: armitage@mpa-garching.mpg.de).

.....

The formation of Uranus and Neptune in the Jupiter–Saturn region of the Solar System

Edward W. Thommes*, Martin J. Duncan* & Harold F. Levison†

* Department of Physics, Queen's University, Kingston, Ontario, Canada K7L 3N6

† Space Studies Department, Southwest Research Institute, Boulder, Colorado 80302, USA

.....

Planets are believed to have formed through the accumulation of a large number of small bodies^{1–4}. In the case of the gas-giant planets Jupiter and Saturn, they accreted a significant amount of gas directly from the protosolar nebula after accumulating solid cores of about 5–15 Earth masses^{5,6}. Such models, however, have been unable to produce the smaller ice giants^{7,8} Uranus and Neptune at their present locations, because in that region of the Solar System the small planetary bodies will have been more widely spaced, and less tightly bound gravitationally to the Sun. When applied to the current Jupiter–Saturn zone, a recent theory predicts that, in addition to the solid cores of Jupiter and Saturn, two or three other solid bodies of comparable mass are likely to have formed⁹. Here we report the results of model calculations that demonstrate that such cores will have been gravitationally scattered outwards as Jupiter, and perhaps Saturn, accreted nebular gas. The orbits of these cores then evolve into orbits that resemble those of Uranus and Neptune, as a result of gravitational interactions with the small bodies in the outer disk of the protosolar nebula.

The most plausible model for the formation of giant-planet cores in the Jupiter–Saturn region is based on the concept of ‘oligarchic’ growth⁹. In this model, the largest few objects at any given time are of comparable mass, and are separated by amounts determined by their masses and distances from the Sun. As the system evolves, the mass of the system is concentrated into an ever-decreasing number of bodies of increasing masses and separations. For a given total mass in the system, the model predicts a relationship between the mass of the largest ‘embryos’ and their number.

In the Jupiter–Saturn region, oligarchic growth breaks down when one or more cores begin to accrete a significant amount of nebular gas, thereby significantly increasing their mass(es) in a short period of time. This is expected to occur when the cores reach about 15 Earth masses⁶ (15M $_{\oplus}$), at which time ‘oligarchic’ growth predicts that the cores will be separated by ~1–2 astronomical units (1 AU is the mean Earth–Sun distance). This in turn implies the existence of between 3 and 5 cores in the Jupiter–Saturn zone (4–10 AU).

As the real Solar System has two gas giants and two ice giants, only two of the cores must have accreted a significant amount of gas. Jupiter was possibly the largest core and the first to accrete gas since it is closest to the Sun, where the disk density was highest and the

formation timescales shortest. Perhaps Saturn's core was larger than the others (due to stochastic variations) and also started to accrete gas at this time, or perhaps Saturn did not accrete its gas until later. In either case, the gas-accreting core(s) increased in mass by roughly an order of magnitude in only 10^5 years (ref. 6). At this point oligarchic growth ceased.

We have investigated the subsequent evolution by performing three sets of numerical integrations. In series I, we assume that the Jupiter and Saturn cores accreted their gas simultaneously. We therefore studied the dynamical behaviour of 2 failed cores of $15M_{\oplus}$ (ref. 6), each initially in circular orbits between fully-formed Jupiter and Saturn. In addition to the planetary-size objects, we included a trans-saturnian disk of smaller objects stretching from 10 to 60 AU from the Sun. In series II and III, we investigated the evolution of a system where Jupiter grows first. In series II, we studied the behaviour of four $15M_{\oplus}$ cores distributed between 5 and 9 AU, where we increase the mass of the inner core to that of Jupiter's in 10^5 years. Series III is similar to series II, except that we studied the behaviour of five $15M_{\oplus}$ cores distributed between 6 and 10 AU in order to explore the hypothesis that one core was lost. (See Methods for a complete description of the simulations.)

In all, we performed eight runs in each series. In four of the series I integrations, both failed cores were scattered into the region beyond Saturn and had their orbits circularized due to gravitational interactions with the disk. The temporal evolution of the run that

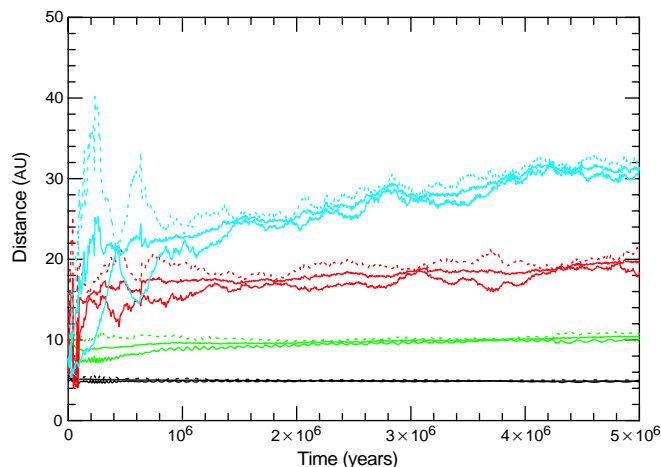


Figure 1 Temporal evolution of model calculations that produced a successful Solar System analogue. Depicted are Jupiter (black), Saturn (green), and the two 'failed cores' (red and blue) in the run which, at its endpoint of 5 Myr, most closely resembles the present Solar System. This run is from series I (see text). Shown are the semi-major axes (thick solid lines) as well as the instantaneous perihelion (thin solid lines) and aphelion (dotted lines) distances of the orbits. Initially the cores suffered multiple gravitational scatterings with Jupiter and Saturn. However, they became decoupled from Jupiter after 9×10^4 years and from Saturn after 2.5×10^5 years. They underwent close encounters with each other until 8×10^5 years. Eventually, the dynamical drag due to small disk objects decoupled them from each other and damped their eccentricities until they were on nearly circular orbits. After this time, they slowly migrated outwards due to the interactions with disk particles. Such a migration has been invoked to explain the structure of the Kuiper belt observed in the real Solar System²¹. At 5×10^6 years the inner core has a semi-major axis, a , of 19.7 AU, an eccentricity, e , of 0.05, and an inclination, i , of 0.2° . For comparison, Uranus currently has $a = 19.2$ AU, $e = 0.006$ and $i = 0.8^\circ$. The outer core has $a = 31.1$ AU, $e = 0.006$ and $i = 0.2^\circ$, and Neptune currently has $a = 30.1$ AU, $e = 0.01$ and $i = 1.7^\circ$. We believe, though, that such a strong correspondence between our model and the real system is largely a coincidence. However, there was one other run in this series that was very similar to the real Solar System (see Fig. S1B in Supplementary Information), so that our mechanism does indeed commonly produce reasonable Solar System analogues. An animation of the dynamical evolution of this system is presented in Supplementary Information.

produced the system that most closely resembles the Solar System is shown in Fig. 1. In seven of the eight series II simulations, all three cores scattered off Jupiter and then evolved onto nearly circular orbits in the outer solar system. In all these cases, one of the cores scattered off Jupiter and evolved onto an orbit near 10 AU, which is the current location of Saturn. That core could subsequently have accreted the amount of nebular gas contained in Saturn. Finally, three of the series III runs produced systems similar to the Solar System. Figure 2 shows 'snapshots' at 5 million years of the system in each series that most closely resembles the Solar System. Similar figures and additional details for all our runs are available; see Supplementary Information.

From our simulations we conclude: first, that this mechanism commonly ($\sim 50\%$) produced reasonable analogues of the real outer planetary system; second, that both 4- and 5-core systems can reasonably reproduce the orbits of the giant planets; and third, that this result seems to be independent of when Saturn accretes its gas.

There is one more issue that must be addressed before we can conclude that we are constructing reasonable analogues of the Solar System. The Solar System is known to have a disk of icy small bodies in nearly circular orbits beyond Neptune, known as the Kuiper belt (shown as small black dots in Fig. 2a; also, see ref. 10 for a review). In order for our mechanism to be applicable to the real Solar System, a similar structure should exist at the end of our simulations. In all our runs there is a population of excited disk objects still encountering the cores (see Fig. 2). These objects should largely be ejected from the Solar System in a few times 10^7 years (ref. 11), and thus are not related to any observed Solar System structure. However, in most of our runs there is a relatively dynamically cold disk that has not been significantly perturbed by the passage of planets—it is this that corresponds to the Kuiper belt. In addition, there is also a population of high-eccentricity objects that are on unstable planet-crossing orbits. This population is similar to the 'scattered disk' recently shown to exist in the Solar System^{12,13}. Thus, our models do indeed produce reasonable Solar System analogues.

A direct comparison between the small-body structures observed in the Solar System and those produced in our simulations is not possible, because there is not yet enough information about the real Kuiper belt. However, we have discovered two previously unknown dynamical processes that helped shape the small-body structures in many of our simulations and which leave well defined dynamical signatures. These may be observed in the real Solar System as the data about the Kuiper belt becomes more complete.

In addition to the scattered disks and 'Kuiper belts' observed in Fig. 2b–d, there is very often a population of excited objects that were perturbed by the planets when the planets were on very eccentric orbits, but which are now beyond the planets' reach. These objects have orbits similar to the scattered disk, but are on stable orbits. As this structure reflects the configuration of the planetary system at early times, we call it the 'fossilized scattered disk'. In addition, in about $\sim 10\%$ of our simulations the objects in the 'Kuiper belt' have had their eccentricities and inclinations excited by the passage of a planet, but not catastrophically so. In these cases, one of the cores was scattered onto a very eccentric, inclined orbit with the semi-major axis $a \gtrsim 60$ AU, which crossed the plane of the system at points both inside and outside the disk, but never actually penetrated the disk. When the core was at the same heliocentric distance as the disk particles it was either above or below the disk due to its inclination. The disk particles were excited by long-range secular effects rather than by gravitational encounters with a planet (see Supplementary Information for some examples).

The idea that the ice giants are failed cores from the Jupiter–Saturn zone represents a significant conceptual shift in our understanding of planet formation. In particular, it suggests that giant-planet formation occurred in a narrow region of the protoplanetary disk, only from ~ 4 AU to ~ 10 AU. Although others have suggested

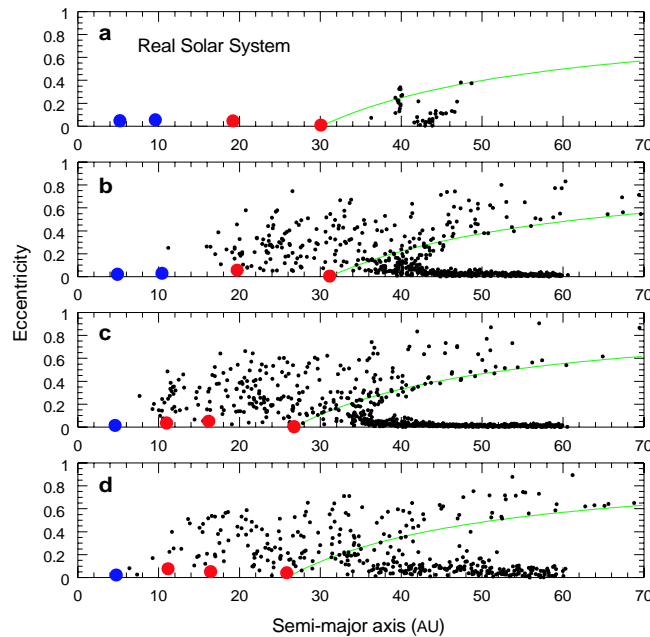


Figure 2 The final orbital elements of most successful runs in each of the three series. For comparison, **a** corresponds to the Solar System, while **b–d** correspond to series I–III, respectively. Eccentricity is plotted versus semi-major axis for the gas giant(s) (blue), the cores (red) and the smaller bodies (black) that originally constitute the planetesimal disk from 10 to 60 AU. These plots were generated 5 million years after the start of the simulation. The green curves show the locus of orbits with perihelion distances at the location of the outer planet. Orbits in the region above and to the left of the green curves are generally unstable on timescales short compared to the age of the Solar System.

Orbits below the green curves are usually stable. An animation of the dynamical evolution of each of these systems is presented in Supplementary Information. In the panel showing the real Solar System, those Kuiper-belt objects which have been observed at multiple oppositions are plotted. The truncation at ~48 AU is probably due to observational bias, as more distant objects are less easily detected. We note that 1996 TL₆₆, thus far the only observed member of the scattered disk population observed at multiple oppositions, is not shown as its semi-major axis is 48 AU.

that Uranus and Neptune formed somewhat inward of their current locations (for example, Neptune at 23 AU) and gently migrated outwards^{14,15}, the model presented here predicts a significantly more compact region of planet formation. Furthermore, it also suggests that our Solar System went through a stage where Uranus and Neptune were violently removed from their primordial orbits by the giant planets and were thrown out to their current locations. This type of instability has been invoked to explain the large eccentricities seen in some other planetary systems^{16–19}; but we believe that ours is the first model that suggests that a similar upheaval took place in the Solar System. □

Methods

We numerically integrated the orbits of our planets, cores, and trans-planetary planetesimal disk particles for 5 million years using our symplectic integrator, SyMBA²⁰. In series I, we included Jupiter, Saturn and two cores. As we expect Jupiter to migrate slightly inwards and Saturn to move outwards during our integrations^{14,15}, we initially placed them at $a = 5.3$ AU and $a = 9.0$ AU, respectively, with eccentricities and inclinations comparable to their current values. The cores were initially located at $a = 6.35$ AU and $a = 7.6$ AU (as predicted by oligarchic growth) on circular, low-inclination orbits. The runs differed only in our choices of the longitudes of the cores, which were randomly distributed. The series II runs initially had four cores at the same locations. The series III runs initially had 15 M_{\oplus} cores at $a = 5.3, 6.24, 7.36, 8.67$ and 10.21 AU.

To make the simulations numerically tractable, for our trans-planetary disk we used bodies, each of mass $0.24M_{\oplus}$, distributed with a surface density proportional to r^{-1} (series I and II) and $r^{-1.5}$ (series III), where r is heliocentric distance. This corresponds to a total disk mass of $216M_{\oplus}$ and $119M_{\oplus}$, respectively, a range consistent with estimates of planetary formation efficiency based on our understanding of the mass of the Oort cloud¹⁵. Initially, the disk particles were on nearly circular, low-inclination orbits. Although we included the gravitational effect of the disk particles on the planets and cores, we ignored self-gravity between the disk particles. In addition, we ignored the dynamical-drag effects of gas. Both these effects would tend to assist the disk in circularizing the orbits of the cores. Therefore, we are underestimating the likelihood that the cores will evolve onto circular orbits in the outer solar system.

In our series II and III runs, we replaced Jupiter and Saturn with cores. The mass of Jupiter (and only Jupiter) was linearly increased to its current mass over a period of 10^3 years. In addition, in series II, we extended the protoplanetary disk inward to 4.5 AU by adding a total of $10M_{\oplus}$ of material between 4.5 and 10 AU.

Received 1 July; accepted 6 October 1999.

1. Safronov, V. S. *Evolution of the Protoplanetary Cloud and the Formation of the Earth and Planets* (Nauka, Moscow, 1969).
2. Wetherill, G. W. An alternative model for the formation of the asteroids. *Icarus* **100**, 307–325 (1992).
3. Chambers, J. E. & Wetherill, G. W. Making the terrestrial planets: N-body integrations of planetary embryos in three dimensions. *Icarus* **136**, 304–327 (1999).
4. Agnor, C. B., Canup, R. & Levison, H. On the character and consequences of large impacts in the late stage of terrestrial planet formation. *Icarus* **142**, 219–237 (1999).
5. Bodenheimer, P. & Pollack, J. B. Calculations of the accretion and evolution of giant planets: the effects of solid cores. *Icarus* **67**, 391–408 (1986).
6. Pollack, J. B. *et al.* Formation of the giant planets by concurrent accretion of solids and gas. *Icarus* **124**, 62–85 (1996).
7. Lissauer, J. J., Pollack, J. B., Wetherill, G. W. & Stevenson, D. J. in *Neptune and Triton* (ed. Cruikshank, D. P.) 37–108 (Univ. Arizona Press, Tucson, 1996).
8. Stewart, G. & Levison, H. F. On the formation of Uranus and Neptune. *Proc. Lunar Planet. Sci. Conf. XXIX*, abstr. no. 1960 (1998).
9. Kokubo, E. & Ida, S. Oligarchic growth of protoplanets. *Icarus* **131**, 171–178 (1998).
10. Morbidelli, A. in *Solar System Formation and Evolution* (eds. Lazzaro, D., Vieira Martins, R., Ferraz-Mello, S., Fernandez, J. & Beauge, C.) 83 (ASP Conf. Ser. 149, 1998).
11. Levison, H. & Duncan, M. From the Kuiper belt to Jupiter-family comets: the spatial distribution of ecliptic comets. *Icarus* **127**, 13–32 (1997).
12. Duncan, M. & Levison, H. F. A scattered disk of icy objects and the origin of Jupiter-family comets. *Science* **276**, 1670–1672 (1997).
13. Luu, J. *et al.* A new dynamical class of object in the outer Solar System. *Nature* **387**, 573–575 (1997).
14. Fernandez, J. A. & Ip, W.-H. Some dynamical aspects of the accretion of Uranus and Neptune—The exchange of orbital angular momentum with planetesimals. *Icarus* **58**, 109–120 (1984).
15. Hahn, J. & Malhotra, R. Radial migration of planets embedded in a massive planetesimal disk. *Astron. J.* **117**, 3041–3053 (1999).
16. Rasio, F. A. & Ford, E. B. Dynamical instabilities and the formation of extrasolar planetary systems. *Science* **274**, 954–956 (1996).
17. Weidenschilling, S. J. & Marzari, F. Gravitational scattering as a possible origin for giant planets at small stellar distances. *Nature* **384**, 619–621 (1996).
18. Lin, D. N. C. & Ida, S. On the origin of massive eccentric planets. *Astrophys. J.* **477**, 781–791 (1997).
19. Levison, H. F., Lissauer, J. J. & Duncan, M. J. Modeling the diversity of outer planetary systems. *Astron. J.* **116**, 1998–2014 (1998).
20. Duncan, M., Levison, H. & Lee, M. H. A multiple timestep symplectic algorithm for integrating close encounters. *Astron. J.* **116**, 2067–2077 (1998).
21. Malhotra, R. The origin of Pluto's orbit: implications for the Solar System beyond Neptune. *Astron. J.* **110**, 420–429 (1995).

Supplementary information is available on Nature's World-Wide Web site (<http://www.nature.com>) or as paper copy from the London editorial office of Nature.

Acknowledgements

We thank G. Stewart and K. Zahnle for discussions, and L. Dones, B. Gladman, W. McKinnon, J. Parker, A. Stern, W. Ward and G. Wetherill for comments on an earlier draft. E.W.T. and M.J.D. were supported by the Natural Science and Engineering Research Council of Canada, H.E.L. was supported by NASA's Planetary Geology & Geophysics, Origins of Solar Systems, and Exobiology programme.

Correspondence and requests for materials should be addressed to M.D. (e-mail: duncan@astro.queensu.ca).

First-order phase transitions in a quantum Hall ferromagnet

Vincenzo Piazza*, Vittorio Pellegrini*, Fabio Beltram*, Werner Wegscheider†, Tomáš Jungwirth‡§ & Allan H. MacDonald‡

* Scuola Normale Superiore and Istituto Nazionale per la Fisica della Materia, I-56126 Pisa, Italy

† Walter Schottky Institute, Munich, Germany

‡ Department of Physics, Indiana University, Bloomington, Indiana 47405, USA

§ Institute of Physics ASCR, Cukrovarnická 10, 162 00 Praha 6, Czech Republic

The single-particle energy spectrum of a two-dimensional electron gas in a perpendicular magnetic field consists of equally spaced energy states, known as Landau levels. Each level is split owing to spin interactions, and its degeneracy is proportional to the magnetic field strength. When the ratio, ν (or 'filling factor'), of the number of electrons and the degeneracy of a Landau level takes an integer or particular fractional values, quantum Hall effects¹ occur, characterized by a vanishingly small longitudinal resistance and a quantized (transverse) Hall voltage². The quantum Hall regime may be used for the controlled study of many-particle cooperative phenomena, such as order-disorder phase transitions (analogous to those observed in conventional magnets). Both isotropic and anisotropic ferromagnetic ground states have been predicted³⁻⁸ to occur in the quantum Hall regime, some of which have been investigated experimentally⁹⁻¹³ in samples with different geometries and filling factors. Here we report evidence for first-order phase transitions in quantum Hall states ($\nu = 2, 4$) confined to a wide gallium arsenide quantum well. We observe hysteresis and an anomalous temperature dependence in the longitudinal resistivity, indicative of a transition between two distinct ground states of an Ising quantum Hall ferromagnet. The microscopic origin of the anisotropy field is identified using detailed many-body calculations.

The study of quantum phase transitions^{14,15}, 'tuned' by system parameters rather than temperature, has enlarged the domain of phase-transition physics. In electronic systems, transitions to ordered ground states can occur when interactions between particles—rather than single-particle potentials—play a dominant role in selecting the ground state. This situation is frequently encountered in the quantum Hall regime owing to the quantization of in-plane kinetic energy into macroscopically degenerate Landau levels. The ordered many-particle ground states discussed originate when two or, in general, N Landau levels are brought close to alignment and the total filling factor of these levels is an integer less than N ^{3,6-8}. The close analogy between these states and those of two-dimensional ferromagnets is often emphasized by using a pseudospin language¹⁶ to describe the Landau level degree of freedom. For the two-level case, we refer to one of the single-particle Landau levels as the pseudospin-up state and to the other as the pseudospin-down state. A general quantum spinor with an arbitrary orientation can be obtained as a linear combination of the up and down states.

Ferromagnetic states are characterized by non-zero pseudospin polarization of the two-component many-particle system, even when the splitting between the two Landau levels vanishes. In single-layer two-dimensional systems at $\nu = 1$, the pseudospin degree of freedom can be the real electron spin. In this case it is rigorously established³ that the ground state is an isotropic strong ferromagnet. In general, the pseudospin degree of freedom can involve real-spin, the cyclotron orbit-radius quantum number, and the layer index in multiple quantum wells or the sub-band index in wide quantum wells⁷. Electron-electron interactions are then expected to lead to tunable pseudospin anisotropy and to a complex range of ordered states which can be explored by adjusting system parameters, often in the same physical sample. In a double-quantum-well structure, for example, Landau level crossings can be accompanied by the introduction of a broken-symmetry phase with easy-plane pseudospin anisotropy whose soft collective excitations and related quantum phase transitions were recently observed¹¹⁻¹³.

The possibility of realizing quantum Hall ferromagnets with the easy-axis (spin aligning along some fixed direction below the critical temperature)—Ising—anisotropy, common in familiar magnetic systems, has also been raised⁵. Experiments¹⁷ on several fractional quantum Hall effect (QHE) transitions suggested interpretations within this framework. However, no rigorous physical picture has been developed to date which is able to describe quantum Hall ferromagnets at fractional filling factors. The experiments reported here reveal intriguing phenomena arising when Landau levels with opposite spin and different sub-band indices are brought close to degeneracy by applying an external electric field. The observed

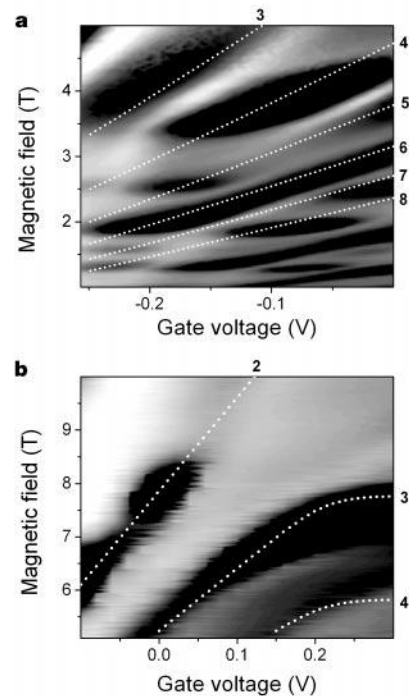


Figure 1 Longitudinal resistivity as a function of the magnetic field and gate voltage. Dark (light) regions represent low (high) resistivity values. The dotted lines show the evolution of the quantum-Hall-effect minima and are labelled by the corresponding filling factors ν . For gate voltages $V_g > -0.26$ V, two sub-bands are occupied: the complex resistivity pattern in this region originates from crossings between Landau levels of the two sub-bands. Similar evolution patterns of the resistivity are obtained in different measurement sessions after thermally cycling the sample. Changes of gate voltages of ~ 20 mV are observed in different measurement sessions owing to small differences in the total electron density. Measurements shown in both **a** and **b** were performed at $T = 330$ mK, with lock-in techniques at a frequency of 12.5 Hz; the a.c. excitation current was set to 100 nA to avoid electron heating.